

ESTIMATING THE VOLUME OF NON-POLAR ICE ON MARS: GEOMETRIC CONSTRAINTS ON CONCENTRIC CRATER FILL ALONG THE MARTIAN DICHOTOMY BOUNDARY. J. S. Levy¹,

C. I. Fassett², and James W. Head³ ¹Oregon State University, Corvallis, OR 97331 (Now at University of Texas Institute for Geophysics) jlevy@coas.oregonstate.edu ²Mount Holyoke College, South Hadley, MA 01075, cfassett@mtholyoke.edu, ³Brown University, Providence, RI 02906, james_head@brown.edu

Introduction: How much non-polar ice is there on Mars? What is the volume of ice in non-polar, ice-rich surface deposits, and what proportion of the martian water inventory do they represent? To answer these questions, numerous geomorphic analyses have mapped the distribution and age of mid-latitude landforms interpreted as indicators of ground ice in the martian subsurface [1-13].

These studies have mapped the spatial relationships between a range of martian landforms interpreted to be not merely ice-rich, but also glacial in origin (formed by flowing ice or deformation of ice and sediment mixtures), notably lobate debris aprons (LDA), lineated valley fill (LVF), and concentric crater fill (CCF). Understanding the age, origin, and distribution of these landforms is important, because, their large aerial extent ($>10^6$ km²) indicates the potential for vigorous glacial activity on Mars. Because crater retention ages for these landforms cluster within ~ 0.1 -1 Ga [8,12,14,15], the ice mass involved in their formation plays a critical role in determining the amount of water in circulation during Amazonian climate evolution. However, no study has fully assessed the volume/mass of ice represented by these landforms or its proportion of the modern water inventory on Mars.

Typically, the uncertainty discussed when describing LDA, LVF, and CCF stems from a lack of information about the internal composition of the landforms. Are these landforms mostly rock/sediment, with interstitial ice pockets (i.e., $\sim 30\%$ ice by volume, typical of terrestrial “rock glaciers”) [3,16-18]? Or are they composed mostly of buried ice with an overlying sublimation lag deposit (i.e., ~ 90 -100% ice, beneath a sediment-rich cover, typical of terrestrial debris-covered glaciers) [19-21]?

Ultimately, if the goal of analysis of LDA, LVF, and CCF is to quantify the amount of ice present in the features (and, accordingly, to quantify the water mass involved in Amazonian climate dynamics and meteorology), then the composition of the features (rock glacier versus debris covered glacier) generates only a small amount of uncertainty in the calculation of martian non-polar ice reservoir volume (approximately a factor of 3: the difference between 30% ice and 90% ice by volume). By far, the most sensitive parameters for determining how much non-polar ground/glacier ice exists on Mars are 1) the aerial distribution of the landforms (how many LDA/LVF/CCF are present at

the surface), and 2) the depth structure of the landforms (how far below the surface the ice extends) [22]. These parameters have the potential to change the calculated non-polar ice reservoir volume by orders of magnitude.

Methodology: Here we present a new approach to estimating the volume of CCF deposits on Mars, based on MOLA-derived martian crater depth/diameter/profile relationships. Several morphometric properties were measured using CTX image data and MOLA gridded topography data for craters containing CCF along the dichotomy boundary (Fig. 1): crater diameter, d , measured crater depth, D_m , and CCF fill radius, r_f . Diameter, d , is measured as the average rim-to-rim distance from two orthogonal MOLA profiles were extracted along cardinal directions for each crater. D_m was measured as the average MOLA elevation of the CCF deposit extracted from two orthogonal profiles along cardinal directions. r_f , half the diameter of the CCF deposit, was measured using CTX image data measured along two orthogonal profiles that span the spatial limit of “brain terrain” surface texture or concentric surface lineations (geomorphic hallmarks of CCF deposits [13]. (Fig. 2)

Using these quantities measured from MOLA and CTX data, relationships between fresh-crater depths and diameters on Mars, coupled with elementary calculus (solids of rotation), permit us to make quantitative estimates of CCF fill volume. The functional relationship between crater diameter (d) and crater depth (D) was quantified by *Garvin et al.* [23]: $d = wD^y$, where w and y are constants that depend on d (all constants reported by [23] vary as a function of d for simple craters, 1-7 km in diameter, complex craters, 7-100 km in diameter, or large craters, >100 km in diameter). The topographic profile of a crater wall follows a similar power-law relationship: here, in Cartesian coordinates of height (y) and radial distance (x): $y = kx^n$ (again, with k and n depending on d) [23]. These simple geometric relationships make it possible to calculate the volume of a CCF deposit, assuming an axially symmetric CCF deposit, by integrating a solid of rotation defined by $y = kx^n$ about the y -axis, and integrating from 0 to $x = r_f$. This technique can be visualized as measuring the volume of stacked disks filling the crater—there is no disk at the very bottom of the crater ($r = 0$), and the disk at the top has a radius of r_f . The volumes of individual CCF deposits were totaled up to calculate the volume of the CCF reservoir

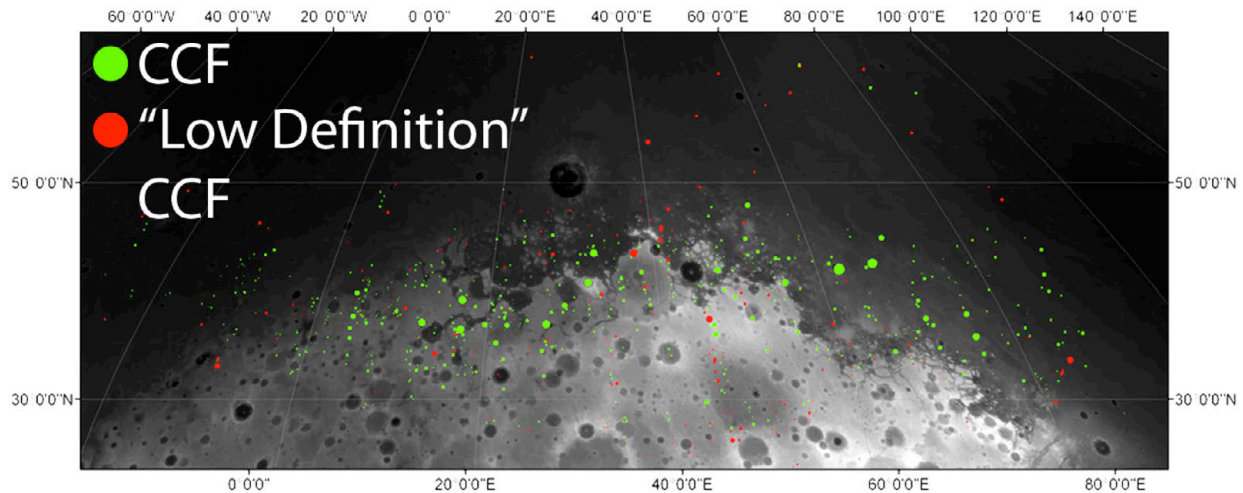


Fig. 1. Map of CCF locations (green dots), and features identified as potentially degraded CCF (red dots). CCF deposits are concentrated between 30-50°N, leading to 30-50° latitude setting the bounding mapping regions for this study. Only CCF (green dots) were considered in this study.

in the mid-latitude study region, and were transformed into minimum and maximum ice masses, by multiplying by 30% and 90% ice volume fractions (rock glacier and debris-covered glacier, respectively) and by assuming negligible ice densification from compaction.

Results and Preliminary Implications: CCF ice volume calculations for this small portion of the martian surface conducted using the methodology described above range from a minimum of $1.2 \times 10^4 \text{ km}^3$ to a maximum of $3.7 \times 10^4 \text{ km}^3$ (assuming rock-glacier ice mixing ratios and debris-covered glacier ice mixing ratios, respectively). Extrapolating these values to the remainder of the mid-latitude CCF-bearing region by extending this CCF volume to the mid-latitude longitudes outside of the study area, yields planet-wide CCF ice volumes spanning from $6.0 \times 10^4 \text{ km}^3$ to $2.0 \times 10^5 \text{ km}^3$. These estimates represent only CCF volumes (and do not include LDA or LVF, which will follow from subsequent analyses). For comparison, observed polar cap water ice volume is $3\text{--}5 \times 10^6 \text{ km}^3$ (24-25), and estimates of latitude-dependent mantle (LDM) ice volume is $\sim 4 \times 10^5 \text{ km}^3$ (22). It is clear from these initial results that martian glacial landforms represent a significant, but previously unquantified component of the global water inventory.

References: [1] R.P. Sharp R (1973), *JGR*, , 78, 4073–4083. [2] S.W. Squyres S.W. (1978) *Icarus*, 34, 600–613. [3] S.W. Squyres SW. (1979), *JGR*, 84, 8087-8096 [4] S.W. Squyres & M.H. Carr (1986) *Science* 231, 249–252. [5] B.K. Lucchitta (1984) *LPSC*, B409–418. [6] V.R. Baker et al. (1991) *Nature*, 352, 589–594. [7] A. Colaprete & B.M. Jakosky BM (1998) *JGR*, 103, 5897–5909. [8] N. Mangold (2003) *JGR*, 108, doi:10.1029/2002JE001885. [9] T.L. Pierce

& D.A. Crown (2003) *Icarus*, 163, 46–65. [10] H. LI et al. (2005) *Icarus*, 176, 382–394. [11] J.W. Head et al. (2006) *EPSL*, 241, 663–671. [12] J.W. Head et al. (2006) *GRL*, 33, doi:10.1029/2005GL024360. [13] J.S. Levy et al. (2010) *Icarus*, 209, 390–404. [14] J.S. Levy et al (2007) *JGR*, 112, doi:10.1029/2006JE002852. [15] W.K. Hartmann & S.C. Werner (2010) *EPSL*, 294, 230–237. [16] R.C. Kochel & R.T. Peake (1984) *LPSC15*, C336–350. [17] W. Haerberli et al. (2006) *PPP*, 17, 189–214. [18] J.L. Piatek (2007) *7th Mars*, Abstr. #3353. [19] M.H. Carr (2001) *JGR*, 106, 23571–23593. [20] N. Mangold & P. AllemandP. (2001) *GRL*, 28, 407–410. [21] J.W. Head et al. (2010) *EPSL*, 294, 306–320. [22] J.S. Levy et al. (2010) *Icarus*, 206, 229–252. [23] J.B. Garvin et al. (2001) *6th Mars*, Abstr. #3277. [24] D.E. Smith et al. (1998) *Science*, 279, 1686-1692. [25] M.T. Zuber et al. (1998) *Science*, 282, 2053-2060.

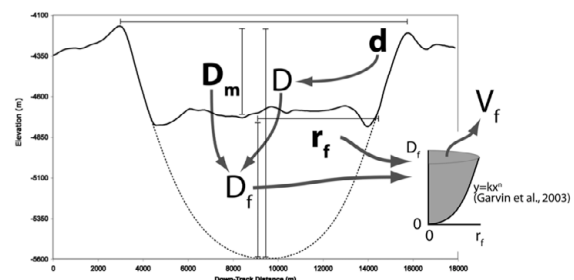


Fig. 2. Schematic illustration of CCF volume calculations.